Best
Available
Copy

AD-772 641

STEROSCOPY OF CONTINUOUS DISTRIBUTION

Nicholas George

California Institute of Technology

Prepared for:

Rome Air Development Center
Advanced Research Projects Agency

November 1973

REPORT DOCUMENTATION PAGE		READ INSTRUCTIONS BEFORE COMPLETING FORM
1. REPORT NUMBER RADC-TR-73-354	2. GOVT ACCESSION NO.	3. RECIPIENT'S CATALOG NUMBER AD 772641
4. TITLE (and Subtitle) STEREOSCOPY OF CONTINUOUS DISTRIBUTION		5. TYPE OF REPORT & PERIOD COVERED Final Technical Report 1 Mar 71 - 30 Sep 73
		6. PERFORMING ORG. REPORT NUMBER
7. AUTHOR(s) Dr. Nicholas George		8. CONTRACT OR GRANT NUMBER(s) F30602-72-C-0021
9. PERFORMING ORGANIZATION NAME AND ADDRESS California Institute of Technology Pasadena, CA 91109		10. PROGRAM ELEMENT, PROJECT, TASK AREA & WORK UNIT NUMBERS 62301D 1057-Project 04-Task 02-WUN
11. CONTROLLING OFFICE NAME AND ADDRESS Defense Advanced Research Projects Agency 1400 Wilson Blvd. Arlington, Virginia 22209		12. REPORT DATE November 1973
		13. NUMBER OF PAGES 47
14. MONITORING AGENCY NAME & ADDRESS(if different from Controlling Office) Rome Air Development Center (OCSE) Griffiss Air Force Base, New York 13441		15. SECURITY CLASS. (of this report) UNCLASSIFIED
		15a. DECLASSIFICATION/DOWNGRADING SCHEDULE N/A

16. DISTRIBUTION STATEMENT (of this Report)

Approved for public release; distribution unlimited.

17. DISTRIBUTION STATEMENT (of the abstract entered in Block 20, if different from Report)

Same

18. SUPPLEMENTARY NOTES
Monitored by:
Joseph J. Simons (OCSE)
RADC/GAFB, NY 13441
AC 315 330-3055

19. KEY WORDS (Continue on reverse side if necessary and identify by block number)
Barium Clouds
Stereoscopy
Photogrammetry

20. ABSTRACT (Continue on reverse side if necessary and identify by block number)
Stereoscopy is applicable to the problem of precisely determining the spatial structure of a photographic record. Using photogrammetric methods, numerical data was obtained for a selected stereo pair of photographs of a barium release cloud produced in the 1971 Secede II test series. The resolution limits of these methods are discussed, based on the inherent limitations of the photographic system. Unresolved problems remaining due to the nature of the photographic image - the cloud itself - are mentioned and a possible path toward their solution is outlined.

DD FORM 1 JAN 73 1473   EDITION OF 1 NOV 65 IS OBSOLETE

STEREOSCOPY OF CONTINUOUS DISTRIBUTION

Dr. Nicholas George

PUBLICATION REVIEW

This technical report has been reviewed and is approved.

Joseph J. Simons
For _Vincent J. Coyne_
RADC Project Engineer

Joseph J. Simons
Contract Engineer

TABLE OF CONTENTS

1. Program Summary

The two main objectives are (1) to develop a theory of photogrammetric measurement for continuously varying contrast distributions and (2) to test our concepts on film of Project Secede Tests supplied via Gerald Meltz of the MITRE Corporation.

For the continuous tone objects, we planned to compare direct parallax measurements made visually on unmodified imagery with those made on imagery which had been artificially contoured using an isodensity recording. The first experiments were done manually, the results being inconclusive largely due to the poor availability of proper stereo-pairs. While at the outset extension of these tests to more precise stereo-plotting equipment had been planned, this did not seem advisable after the preliminary parallax measurements had been made, and further effort on the project was terminated. The detailed technical findings are included in the following text.

The figures appearing in this report do not follow in numerical sequence.

1

2. Technical Discussion

2.1 Stereoscopy

Stereoscopy is applicable to the problem of precisely determining the spatial structure of a photographic record. Using the standard photogrammetric methods described in Section 2.2, numerical data is obtained for a selected stereo pair of photographs of a barium release cloud. The resolution limits of these methods are discussed based on the inherent limitations of the photographic system. Problems remaining due to the nature of the photographic image - the cloud itself - are mentioned and a possible path toward their solution is outlined.

The procedure leading up to the actual application of the parallax measurements is as follows. A sequence of seven frames was selected from the 35mm color Spruce footage. A sequence was chosen in which the shape of the cloud was relatively well defined and the striations pronounced. The frames in this sequence were then prepared for use in a stereo viewer. By a stereo visual inspection of various combinations of pairs from the sequence, a single pair was chosen for the work which followed. The frames which made up this stereo pair had been separated by three frames in the original footage, thereby implying a time lapse of 30 seconds. The frame which was chronologically first in the sequence became the right member of the pair and the later frame became the left member. This choice is not arbitrary as becomes apparent in Section 2.2.

The continuously contrast varying transparencies were converted into quantized feature data using a Joyce-Loebl/Technical Operations

2

Isodensitometer. The resulting left and right isodensity recordings are reproduced in Figures 1a and 1b respectively. The isodensity contours were enlarged by a factor of 20-to-1 over the 35mm transparencies which allowed the recording of the entire cloud on a single sheet; however, recording ratios up to 1000-to-1 are possible. The scanning spot during the recording was a square 80μ by 80μ; considerably higher resolution is possible as is mentioned in Section 2.3.

Besides the quantative measurements of the isodensity recordings, several tracings were made of the recordings and prepared for stereo viewing. This was done in an effort to obtain qualitative visual information from the isodensity recordings. These tracings are shown in figure 2. The first such pair (figure 2a and b) resulted in a confused image when viewed in stereo. The later traced pairs (figures 2c and d and 2e and f) produced a slight three dimensional effect when viewed in stereo but did not yield any real "depth" information about the image.

2.2 Photogrammetry of Isodensity Recordings of Barium Ion Clouds

In considering the subject of stereoscopy we will treat both cases in which a stereo pair is produced (a) from multiple camera site photographs and (b) from images recorded by a single camera at different times.

For the case of multiple camera sites we refer to figure 3. The point P is imaged at points y_a and y_b on films A and B respectively. By using geometrical optics we obtain the following relationships which form the basic equations of photogrammetry:

(a)

(b)

(c)

(d)

(e)

(f)

Figure 2

4
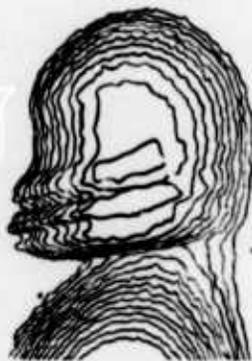
$$\tan \theta_a = \frac{y_a}{S_f} = \frac{y_a{}'}{S'} = \frac{d_\infty + y_b{}'}{S'} \qquad (1)$$

$$\tan \theta_b = \frac{y_b}{S_f} = \frac{y_b{}'}{S'} \qquad (2)$$

An expression for the distance from the lens plane to the point P is

$$S' = \frac{S_f\, d_\infty}{p} \approx \frac{f\, d_\infty}{p} \qquad (3)$$

where p is the parallax of the point P and is defined by

$$p = y_a - y_b$$

For the case of two point images at distances $S_1{}'$ and $S_2{}'$ from the lens plane, it can easily be shown from equations (1) and (2) that

$$S_2{}' - S_1{}' = \frac{S_1{}'(p_1 - p_2)}{p_2} \qquad (4)$$

where p_1 and p_2 are the parallax of points P_1 and P_2 (not shown in figure 3) respectively.

The same principles apply in the case of a pair of photographs from a single camera when the camera is moved a distance d_∞ in the plane of the lens during the time inverval between the two exposures. Relatively, an equivalent pair of photographs results if the object moves a distance $-d_\infty$ with respect to a stationary camera during the same time interval. We wish to consider an object moving with velocity $\underline{v}$ with respect to a

5

Figure 3

A. Position of Camera at time $t_2 > t_1$

B. Position of Camera at time t_1

Figure 4

6
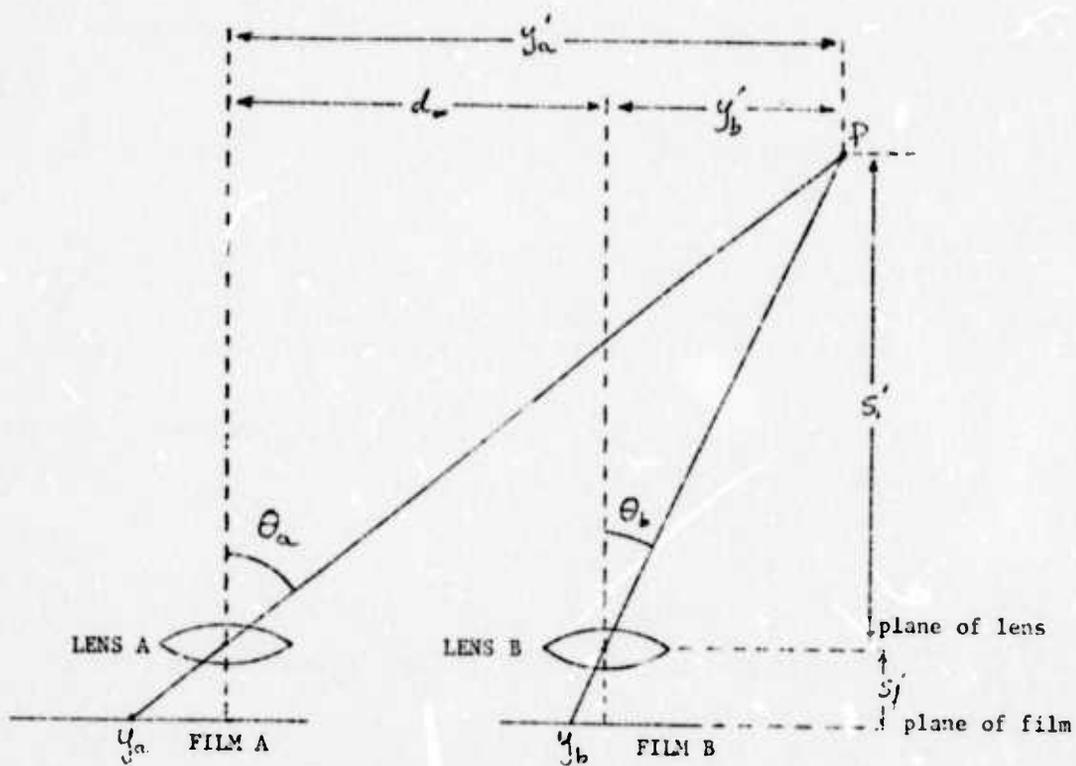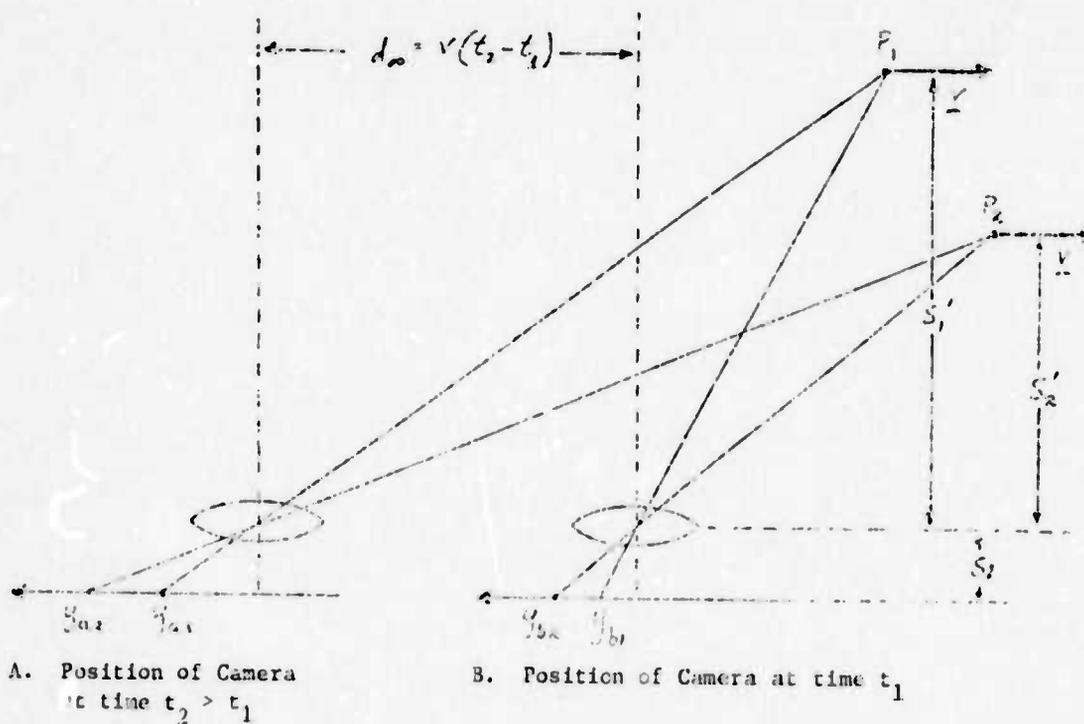
stationary camera and for simplicity we assume for the present that

$$\underline{v} \cdot \underline{n} = 0 \qquad\qquad (5)$$

where $\underline{n}$ is the unit normal to the lens.

In figure 4, points P_1 and P_2 are moving to the right and A and B are the positions of the camera (relative to P_1 and P_2) at times t_2 and t_1 respectively (where $t_2 > t_1$). The analysis is now the same as in the two camera case of figure 3. We see that equations (1) through (4) still apply but now $d_\infty = v(t_2 - t_1)$.

Figure 5 illustrates the fact that in the stereo viewing of transparencies produced by the systems of figure 3 or 4, a definite right-to-left relationship exists between the members of the stereo pair. The image produced at point A becomes the left member of the stereo pair while that produced at point B becomes the right member. If the transparencies are interchanged by translation only, the distances S_1' and S_2' will appear inverted. The same principle applies in making parallax measurements and must be taken into account when we calculate normal distances from photographs or isodensity recordings made from a stereo pair.

We can determine the corresponding azimuthal coordinate of the object point by first measuring the position of the object point on either view of the stereo pair. Then using equation (1) or (2), whichever is appropriate, we can calculate the corresponding object coordinate using the value of S' calculated from equations (3) or (4).

7
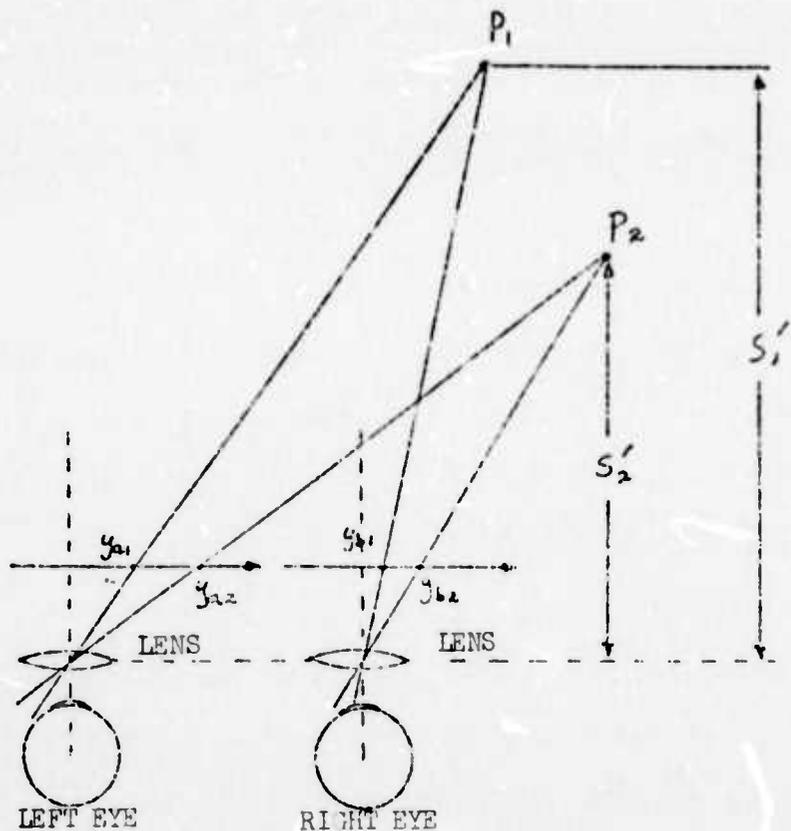
Figure 5

Twenty points were used in the photogrammetry; of these, six typical points are shown in Fig. 1a and 1b. The star points are labeled with an S. The points selected for this analysis lie in the striated portion of the cloud and are numbered as follows: points 1 through 5 and 11 through 15 lie along the dark or higher optical density bands which mark the striations; points 6 through 12 and 16 through 20 lie on the lighter or lower optical density bands. The points A,B and C represent stars in the background sky; since these can be considered to lie at an infinite distance from the camera, they have a parallax $p = 0$ and can be used as reference points in each view.

8
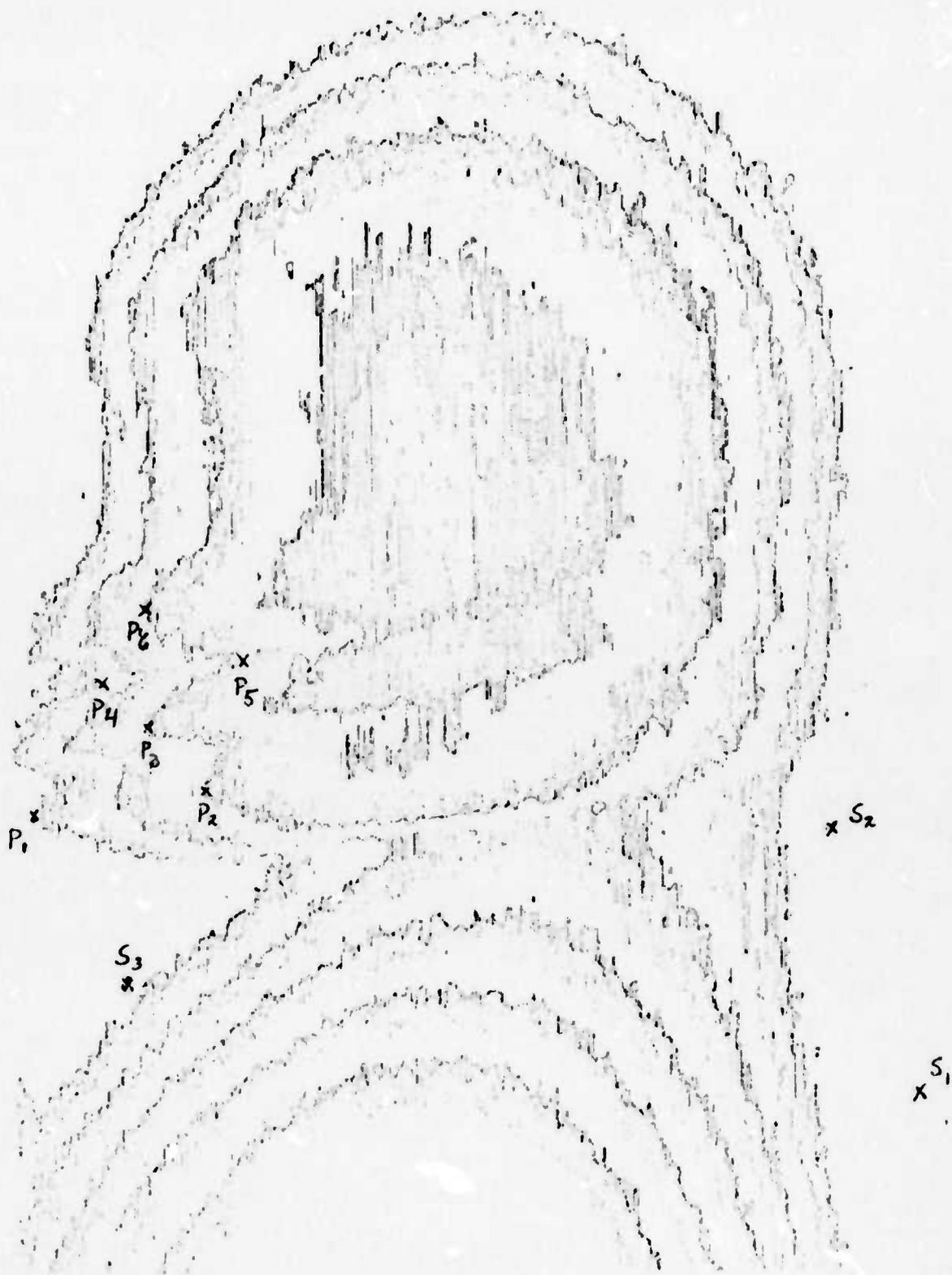
Figure 1a: Isodensity trace of left view

9
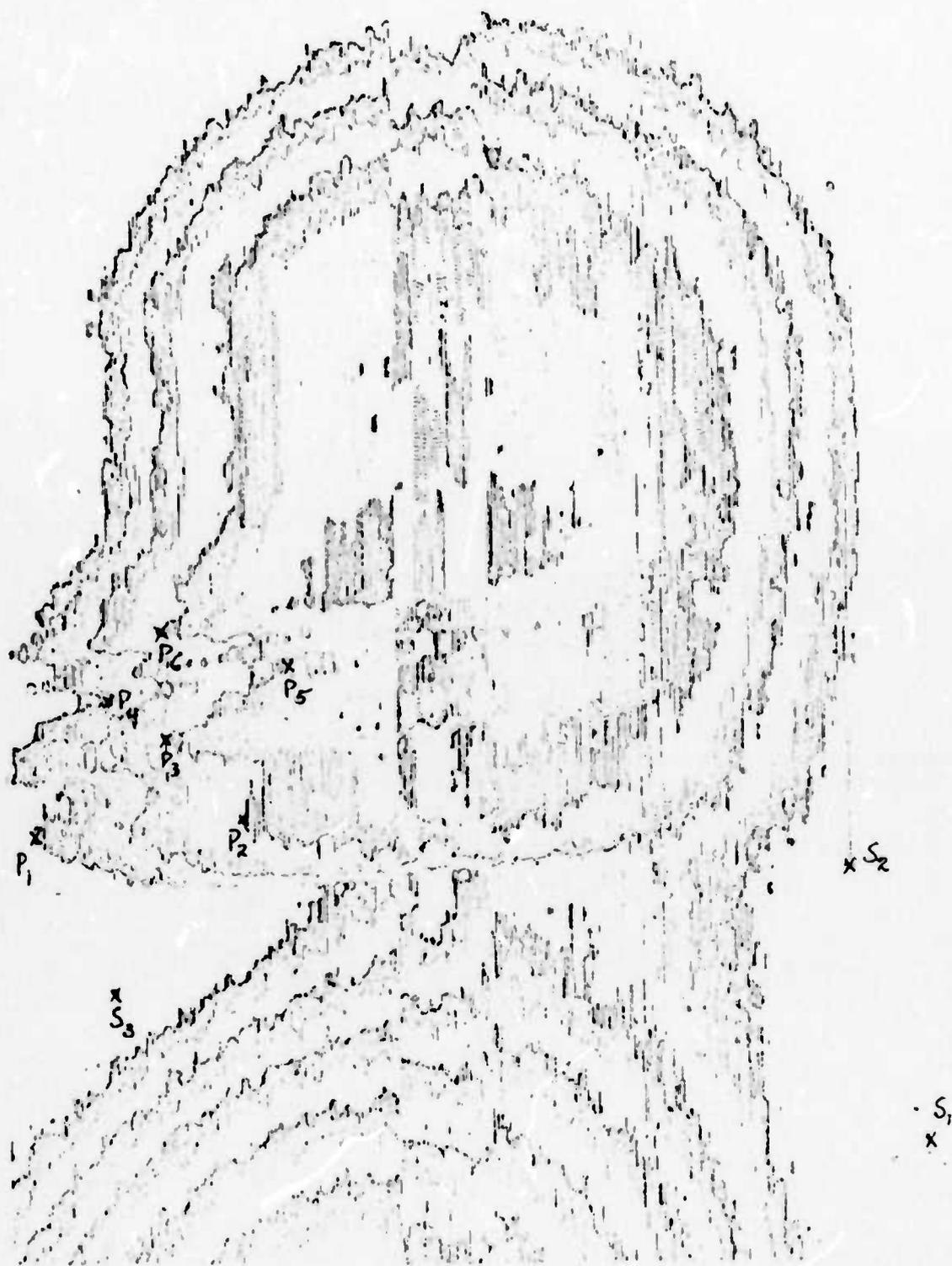
Figure 1b: Isodensity recording of right view

Referring now to figure 6a we see a field of numbered vectors which represent the change in position of each of the points. The tip of each vector is the location of the corresponding point in the left view (figure 1a) and the tail locates the position of the point in the right view (fig. 1b). Unfortunately we see that the vectors are not all parallel as was implicitly assumed in the discussion of section 2.2. We will consider the problem of errors introduced by local variations in velocity in Section 2.5.2. For now we will consider only the projection of each vector in some average direction which we will call the y-axis. The direction of this axis is taken to be antiparallel to the direction of the cloud velocity which we approximate by the following averaging method. The vector field of figure 6a indicates the direction of the velocity of each point but gives no information regarding the magnitude of the velocity. However our stereoscopic analysis assumes that these magnitudes are equal. As a first-order approximation we sum twenty vectors of equal magnitude (as shown in figure 6b) whose directions are those of the corresponding vectors in figure 6a; we take the direction of the resultant to be an approximation to the direction of cloud travel.

Since the parallax of each point is

$$p = y_a - y_b = y_{left} - y_{right}$$

We can now determine the value of p_n for the nth point by measuring the length of the projection of the nth vector onto the y-axis. We see in table I that the parallax of point #8 is near the average for the set.

11
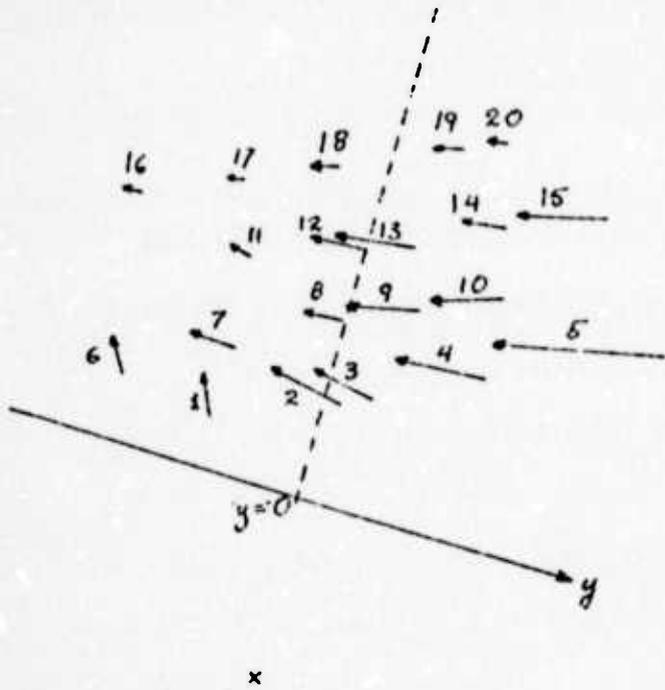
Figure 6a: Vectors connecting points in left and right views
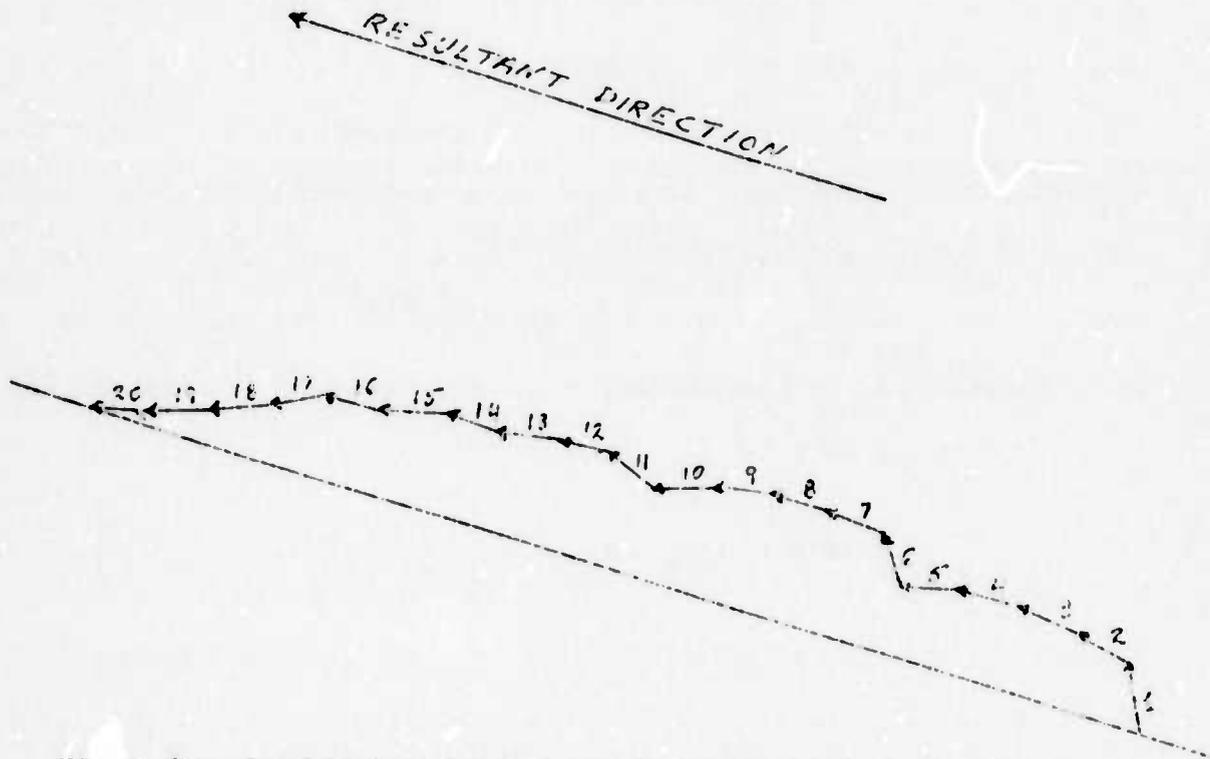
Figure 6b: Graphical approximation of direction of cloud travel

We can rewrite equation (4) in the following way:

$$S_n' - S_8' = \frac{S_8'(p_8 - p_n)}{p_n}$$

or

$$S_n' = \frac{S_8'(p_8 - p_n)}{p_n} + S_8' \tag{6}$$

Assuming that point #8 lies at a distance of 100 km from the camera we set $S_8' = 100$ km and compute the distances of the remaining points using eqn. (6). The results are shown in table I.

2.3 Error Analysis

Errors in determining the exact location of a point from a stereo pair of images of the plasma cloud are due to the following:
(1) Resolution limits of the systems used to record and process the imagery. (2) Variation of the shape of the cloud. (3) Uncertainty in location of corresponding points in the two stereo views. Of these, (1) is independent of the nature of the imagery itself; and (2) and (3) are directly related to the nature of the object, namely the plasma cloud.

2.4 Resolution and Diffraction[3]

Because lens diffraction and film resolution cause each image point to be spread out into a spot on the photographic record there is a limit to the precision with which the position of points can be measured on the photographic image. It follows that there will be a corresponding error in the determination of the distance S' from a stereo pair.

n	p_n (mm)	S_n' (km)	
1	-2.4	225	
2	-9.4	57	
3	-8.7	62	Group 1 (dark band)
4	-11.9	45	
5	-22.5	24	
6	-2.3	235	
7	-4.7	115	
8	-5.4	100	Group 2 (light band)
9	-9.3	58	
10	-9.4	57	
11	-2.4	225	
12	-6.7	81	
13	-9.0	60	Group 3 (dark band)
14	-7.0	77	
15	-11.6	46	
16	-3.4	159	
17	-1.3	416	
18	-3.4	159	Group 4 (light band)
19	-4.0	135	
20	-2.5	216	

$p_{average}$ = -5.9

Table I

14

We can obtain expressions for diffraction errors from eqs. (1), (2) and (3) by differentiation.

For image points inclined at an angle θ (shown in figure 3) to the lens optical axis, the spread δy recorded on the film plane due to diffraction is

$$\delta y = \frac{f \delta \theta}{\cos^2 \theta} \tag{7}$$

where f is the lens focal length. Thus the maximum possible uncertainty in parallax p for a stereo pair (assuming $\delta \theta_a = \delta \theta_b$) is

$$\delta p = \delta y_a + \delta y_b = f \delta \theta \left(\frac{1}{\cos^2 \theta_a} + \frac{1}{\cos^2 \theta_b} \right) \tag{8}$$

This uncertainty in parallax then gives a maximum uncertainty $|\delta S'|$ in the photogrammetrically calculated altitude

$$|\delta S'| = \frac{f d_\infty \, \delta p}{p^2} = \frac{(S')^2 \delta \theta}{d_\infty} \left(\frac{1}{\cos^2 \theta_a} + \frac{1}{\cos^2 \theta_b} \right) \tag{9}$$

The error introduced by diffraction in the azimuthal coordinate becomes, to first order at least,

$$|\delta y_a'| = |\delta y_b'| = \frac{S' \, \delta \theta}{\cos^2 \theta} \tag{10}$$

The angular uncertainty $\delta\theta$ is given by

$$\delta\theta = \frac{1}{wf} + \frac{2\lambda}{\pi D} \tag{11}$$

where w is the film resolution in cycles/mm, f is the lens focal length, λ is the wavelength of the light, and D is the diameter of the camera aperture. If we assume a photographic system in which $f = 50$ mm, $w = 50$ cycles/mm, $D = f/1.4$, $\delta\theta = 0.4 \times 10^{-3}$ radian.

Table II shows the optimum limits of resolution for the system indicated above, a typical cloud altitude of $S' = 100$ km, cloud velocity of 70 m/sec, and an interval between exposures of 30 sec. The parameters ℓ_0 and ℓ_1 referred to in table II are characteristic lengths which indicate the degree of resolution attainable in altitude and azimuth. Figure 7 shows schematically how these parameters apply to the detail structure of the ion cloud. Note that the values of ℓ_0 and ℓ_1 calculated in table II refer to a 30 sec time lapse. A longer time interval yields a proportionally higher degree of resolution.

Figure 7

16
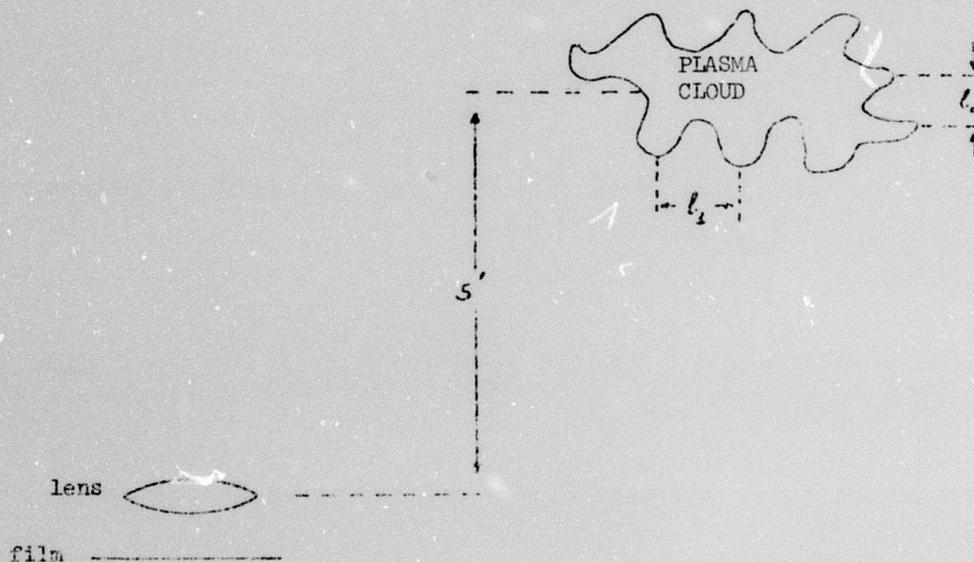
Factors Influencing Quantitative Stereo-Analysis of Barium Ion Cloud

Item	Algebraic form of error term	Resolution for system described in section 3.1
1. Camera resolution, $\delta\theta$ (film and diffraction)	$\dfrac{1}{wf} + \dfrac{2\lambda}{\pi D}$	0.4×10^{-3} radians
2. Altitude resolution, ℓ_0	$\dfrac{(S')^2 \, \delta\theta}{d_\infty} \left(\dfrac{1}{\cos^2\theta_a} + \dfrac{1}{\cos^2\theta_b} \right)$	4 km
3. Azimuthal resolution, ℓ_1	$\dfrac{S' \, \delta\theta}{\cos^2\theta_{min}}$	40 m
4. Shape variation in cloud a) Uniform expansion	correctable ± 10%	
b) False parallax from differential shape change	$\dfrac{S' \, \delta v}{v}$	

Table II

17

2.5 Shape Variation of Cloud

Two difficulties arise in parallax measurements of a stereo pair due to the change in the shape of the cloud. These can be attributed to (1) uniform expansion of the cloud and (2) differential shape change.

2.5.1 Uniform Expansion[4]

If the ion cloud expands uniformly there is an inward drift velocity toward the camera and therefore eqn (5) is no longer true. This being the case, one would expect that severe errors might be introduced.

A laboratory experiment was conducted to assess this effect. Using the three-dimensional styrofoam model with "pencil-rod" features (shown in figure 8) a stereo pair was made corresponding to a base line separation of 15 miles. A series of progressively larger and smaller prints were made of only one photograph of the pair; these were viewed with the fixed-scale left band member. No undue difficulty was observed with scale changes to ±10%. In our data reduction we can correct for this effect by using a different lens-to-transparency distance for the left and right members of the pair.

2.5.2 Differential Shape Change[5]

This effect appears to contribute a relatively serious error to the photogrammetry from successive time-elapse photographs. To estimate the effect we suppose some element of the ion cloud has a velocity different from the drift velocity by an amount dv. By differentiation

Figure 8

19
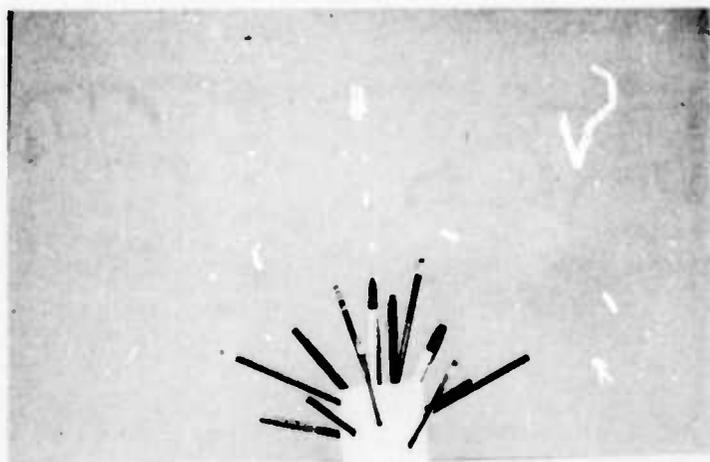
of eqn (3) we find:

$$dS' = \frac{fd_\infty \, dp}{p^2} + \frac{f}{p} \, (vdt + tdv) \tag{12}$$

where the first term on the right is the elevation uncertainty of equation (9). The first term in parentheses is equal to zero in the case of a stereo pair since t is constant for all image points. The false parallax due to shape changes therefore reduces to

$$dS' = \frac{ftdv}{p} \tag{13}$$

$$dS' = \frac{S'dv}{v} \tag{14}$$

For $v = 70$ m/sec and a fluctuation locally of $dv = 5$ m/sec we find an error $dS' \simeq 10$ km. In the case of photographs taken from an aircraft in steady flight. the v in ean. (14) is large and the resultant error varying as the ratio $\frac{dv}{v}$ is decreased.

2.6 Uncertainty in Location of Corresponding Points in the Two Views

For the purpose of calculating the altitude of a point from a stereo pair of images it is of major importance that we be able to identify and locate accurately the corresponding points on both views. Upon viewing the photographs of the plasma cloud it is easy to identify outstanding features such as the striations. One can even estimate visually the center of the striations at a given point but the intensity

20

of the photograph is too smoothly varying to allow a very accurate visual estimation. It is certainly not accurate enough to resolve the change of position with respect to the two views for a point on the cloud. The isodensity traces on the other hand afford a means of associating limiting contours with the features of the object and thus a clue in identifying individual points. For the calculations of section 2.2 the points were located by making the tentative assumption that corresponding points in the photographs map into points of equal density on both isodensity recordings. A point was then located in both views by selecting a point on a contour in one view and then finding its apparent image on the contour representing the same density in the other view. Of course there still remains some uncertainty in the location of a given point but we now have a means of making a much better approximation than was available with the photographic records. The errors due to uncertainty in the location of corresponding points will have the same algebraic form as ean (12):

$$|\delta S'| = \frac{f d_\infty \, \delta p}{p^2} \quad .$$

2.7 Discussion of Results

In view of the discussions of photogrammetry and error analysis some comments can now be made regarding the calculated data found in table I. Some of the S_n values in the table can be seen to contain large and obvious errors.

Referring to figure 6a we see that vector 17 is very small; since the scale at which the measurements were made is the same as that of figure 6a, it is reasonable to assume that point 17 is an error due to poor precision. This sort of error can be minimized by making the measurements on an enlargement of the original stereo isodensity recordings.

It is possible that points 1, 6, and 11 also suffered from lack of precision since the projections of their vectors along the y-axis (in figure 6a) are small. However, these three vectors also indicate a differential shape change at those points. Each of these vectors has a component perpendicular to the y-axis which is comparable to the y-directed component. This introduces an uncertainty in the magnitude of the corresponding velocity vector which is comparable with the magnitude of the velocity itself. i.e., δv is of the same order as v. From eqn. (14) we see that this suggests a possible error of the order of 100% for these points.

Disregarding points 1, 6, 11 and 17 in table I and considering the remaining points it is obvious that the size of the cloud implied by this data is several times larger than the actual dimensions. The values in table I should be clustered more tightly around the 100 km value which implies that the vectors in figure 6a should be more nearly equal in length. This would seem to imply that we have made an error in the attempt to locate corresponding points on the left and right isodensity recordings. This in turn would imply that the assumption mentioned in section 2.6 is not valid. Clearly, if parallax measurements are to yield reliable numerical results, another method of accurately

22

locating a point in both views of the stereo pair must be tried.

It is now apparent that the image points represented by an iso-density contour in one view are not necessarily represented by a contour of equal density in the other view. This could be due, in part at least, to an overall decrease in optical density resulting from the uniform expansion of the cloud. (Note that this would not apply to stereo pairs obtained from multiple cite cameras.) In this case we might take as a new trial assumption the following: that a set of image points corresponding to an isodensity contour in one view is represented by some isodensity contour on the other. If this is so, then we can attempt to match corresponding pairs of contours on the two density recordings. Once this is done, corresponding points can be located on the appropriate pairs of contours and the photogrammetric process proceeds as usual. The matching of contours could be accomplished by cross-correlating the shapes of various pairs of contours and matching the pair for which the correlation is a maximum. Unfortunately it would be difficult at best to do this visually. However, such a cross-correlation process could be done with a high degree of accuracy using optical processing.

2.8 Conclusion

We have seen in sections 2.3, 2.4, 2.5, 2.6 that a reasonable degree of resolution can be attained in locating both altitude and azimuthal coordinates of an object using standard photogrammetry techniques. A major factor in achieving such resolution, however, for the case of the plasma cloud is the accuracy with which an image point can be

identified and located in both views of the stereo pair. Visual examination of the photographic records and even of the isodensity recordings failed to give the required accuracy in point location. It appears, however, that the production of a stereo pair of isodensity recordings from the photographic pair is a good initial step in solving the problem. A higher level of sophistication in further processing of the isodensity recordings has been suggested involving cross-correlation of the individual contours in the stereo pair. Unless a solution to the problem of accurate point location is found, the photogrammetric methods outlined herein will not yield satisfactory numerical values for object coordinates.

REFERENCES

1. N. George and J. McCrickerd, Holography and Stereoscopy: The Holographic Stereogram, pp. 343-4.

2. N. George et al, Photogrammetry of Barium Clouds, California Institute of Technology, March 1971, pp. 5-6.

3. Ibid., pp. 7-9.

4. Ibid., p. 12.

5. Ibid., pp. 12-13.

3. Research Personnel, References, Acknowledgment

3.1 Personnel Who Participated in this Research Program

Name	Classification
Dr. Nicholas George	Principal Investigator
Dr. R. B. MacAnally	Senior Research Fellow
Christian Juvan	Junior Electrical Engineer
R. E. Gray	Doctoral Scholar
A. C. Livanos	Doctoral Scholar

3.2 Consulting Personnel Who Participated (at no direct cost to the subject contract)

Name	Organization
Gerald Meltz	The MITRE Corporation Bedford, Massachusetts
Dr. R. P. Porter	Woods Hole Oceanographic Laboratories Woods Hole, Massachusetts

3.3 Acknowledgment and References

Helpful participation by G. Meltz and R. P. Porter is acknowledged. Also some references of particular interest in connection with this work are the following:

1. "Holography and Stereoscopy: The Holographic Stereogram," Nicholas George and T.J. McCrickerd, Photographic Sci. and Engin. 13, 342 (1969).

2. "Photogrammetry of Barium Clouds," Nicholas George, R. P. Porter, R. B. MacAnally and Gerald Meltz, Caltech Report submitted to the MITRE Corp, March 1971.

3. "Three-Dimensional Structure of Continuous-Tone Objects by Stereo-Photogrammetric Techniques," R. P. Porter, The MITRE Corp., Unpublished memo.
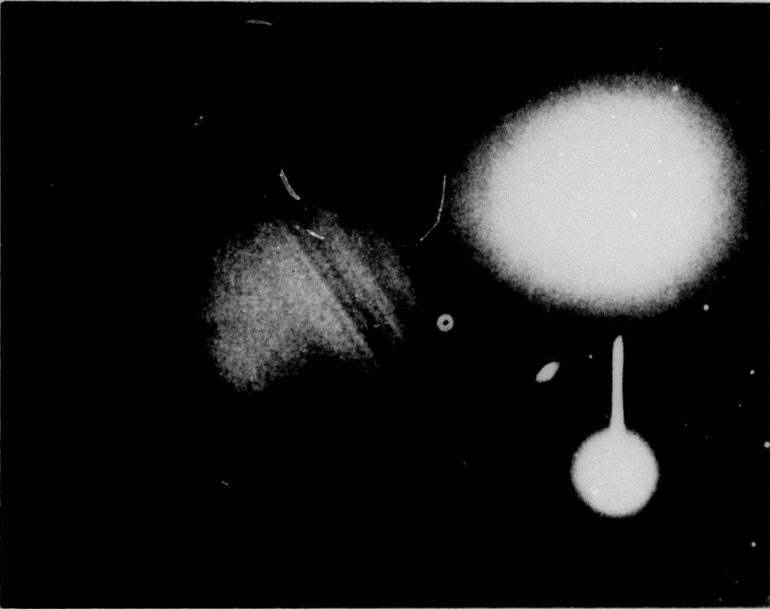
FRAME   1
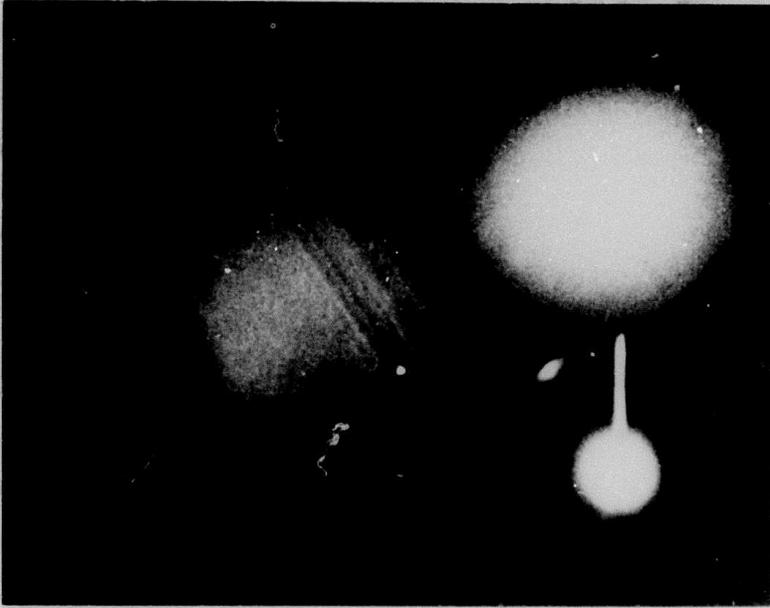
FRAME   2

A-1 Original set of seven frames from the 35 mm spruce footage. Frame 1
and frame 4 were used for the photogrammetric calculations.

FRAME 3

FRAME 4

Figure A-1 continued

29

FRAME 5

FRAME 6

Figure A-1 continued

30
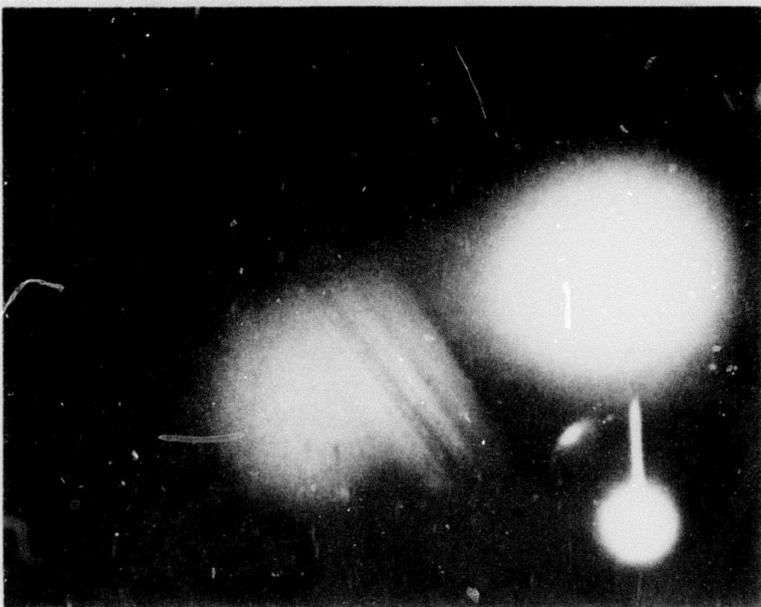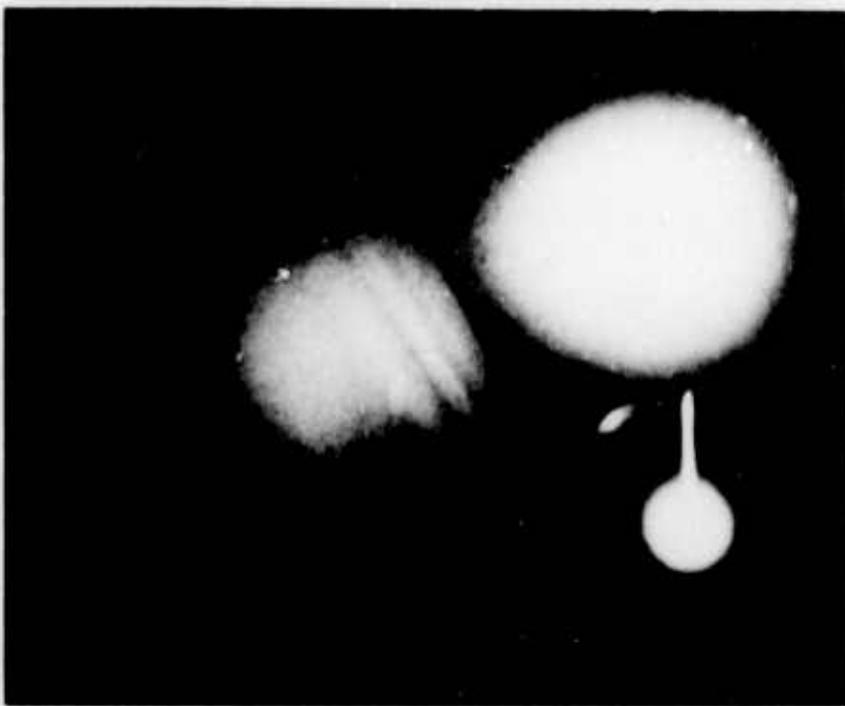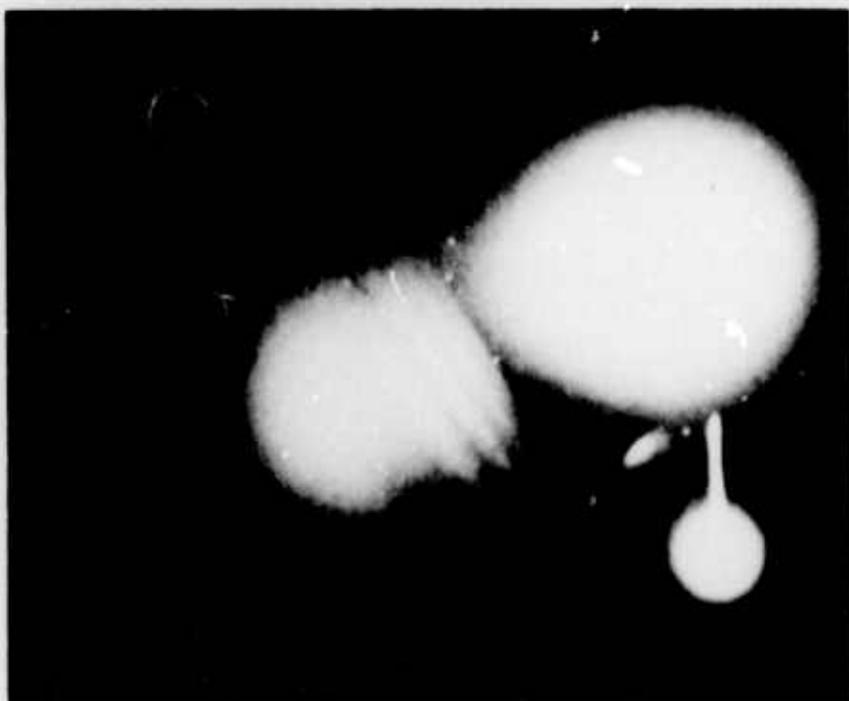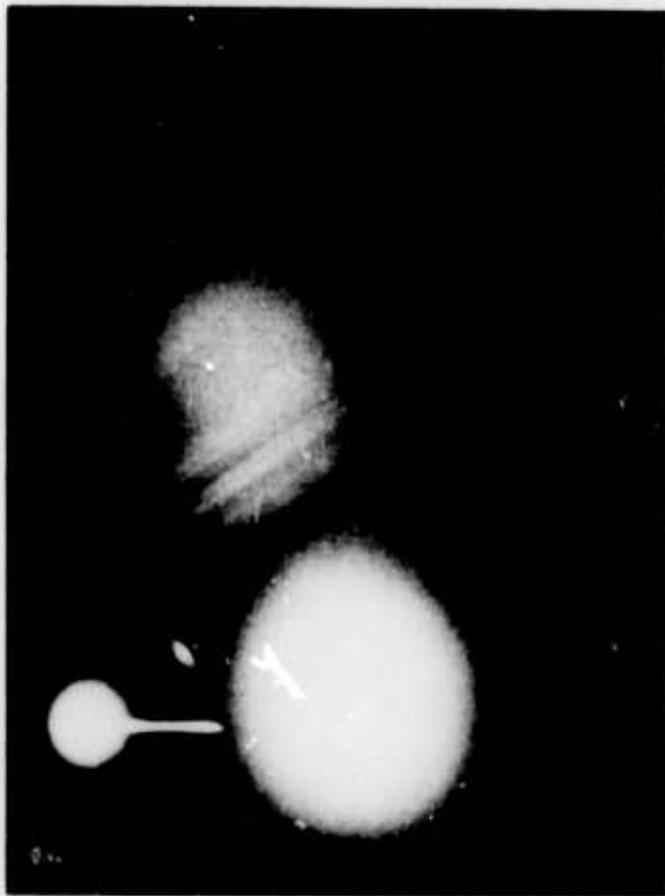
FRAME   7

Figure A-1 continued
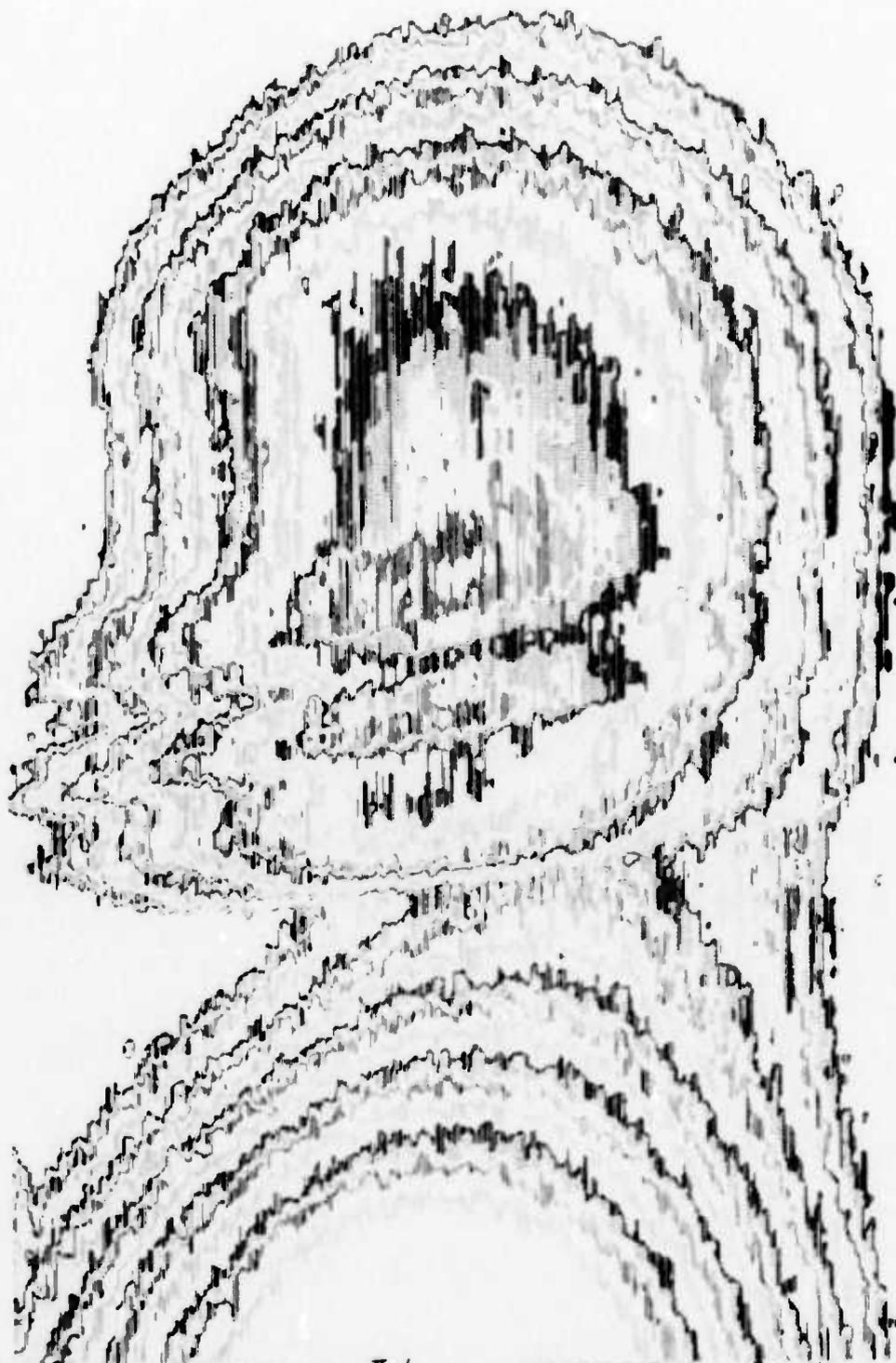
A-2   Isodensity trace of left view made by a Joyce-Loebl/Technical
Operations Isodensitometer. Note that isodensity contours
were enlarged by a factor of 20-to-1 over the 35 mm transparencies.

DATE 9-11-72   RECORDING NO. II-1   IDENTIFICATION   2ND VIEW, LEFT (FRAME 4)

SPOT HEIGHT	1 mm	WEDGE NUMBER	8636	RATIO ARM	20:1	OPERATOR
SPOT WIDTH	1 mm	Δ D INCREMENT				COMMENTS:
OBJECTIVE	16 /	TABLE SPEED	20 in/m	RECORD SPACING	375μ
CONDENSER	X /	PEN DAMPING		SAMPLE SPACING	18.75μ

32
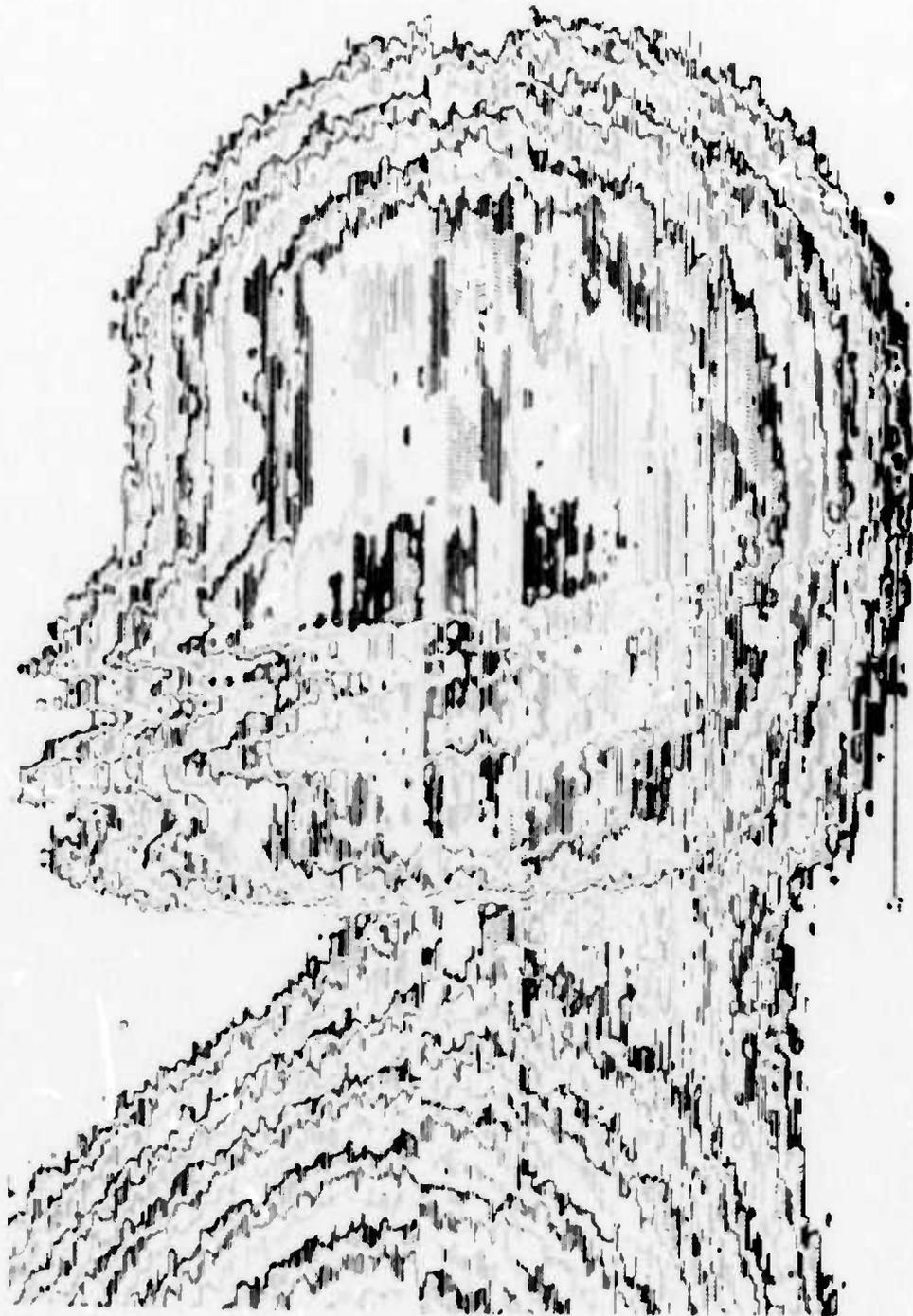
A-3 Isodensity trace of right view, made in the same fashion as A-1. Note furthermore that in both traces a 80μ by 80μ scanning spot was needed; considerably higher resolution is possible, but that would not make the point correspondence any easier.

DATE _____ RECORDING NO. _II-R_ IDENTIFICATION _2ND VIEW, RIGHT (FRAME 1)_

SPOT HEIGHT _1 mm_	WEDGE NUMBER	_B 626_	RATIO ARM	_20:1_	OPERATOR _____
SPOT WIDTH _1 mm_	Δ D INCREMENT				COMMENTS: _____
OBJECTIVE _X6_ /	TABLE SPEED	_30 /min_	RECORD SPACING _375μ_		_____
CONDENSER _X_ /	PEN DAMPING		SAMPLE SPACING _187.5μ_		_____

A-4   Heavy contour tracing of left view.
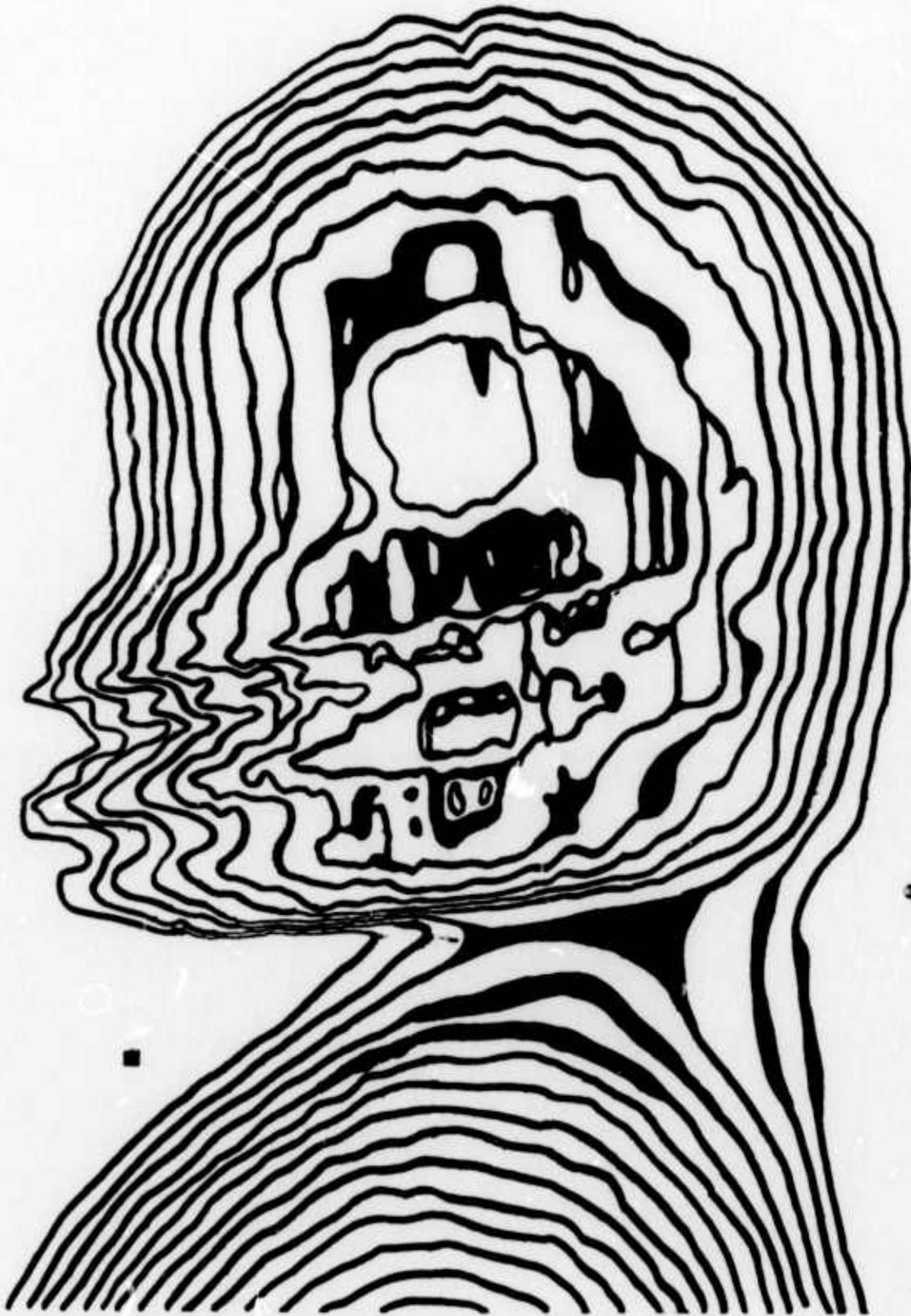
A-5   Heavy contour tracing of right view. When A-3 and A-4 were
       viewed in stereo a confused image resulted.
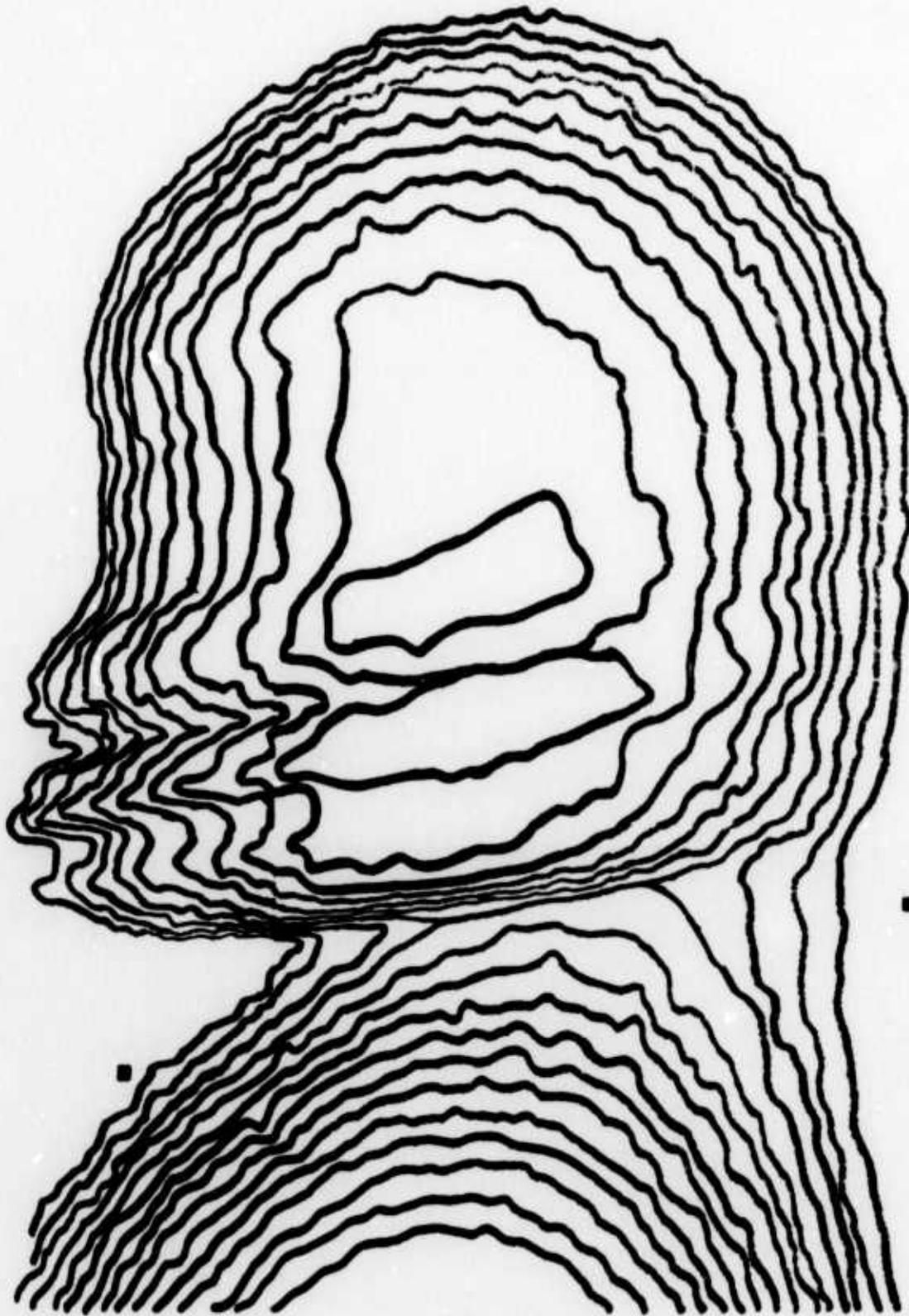
A-6   Light contour tracing of left view.

36
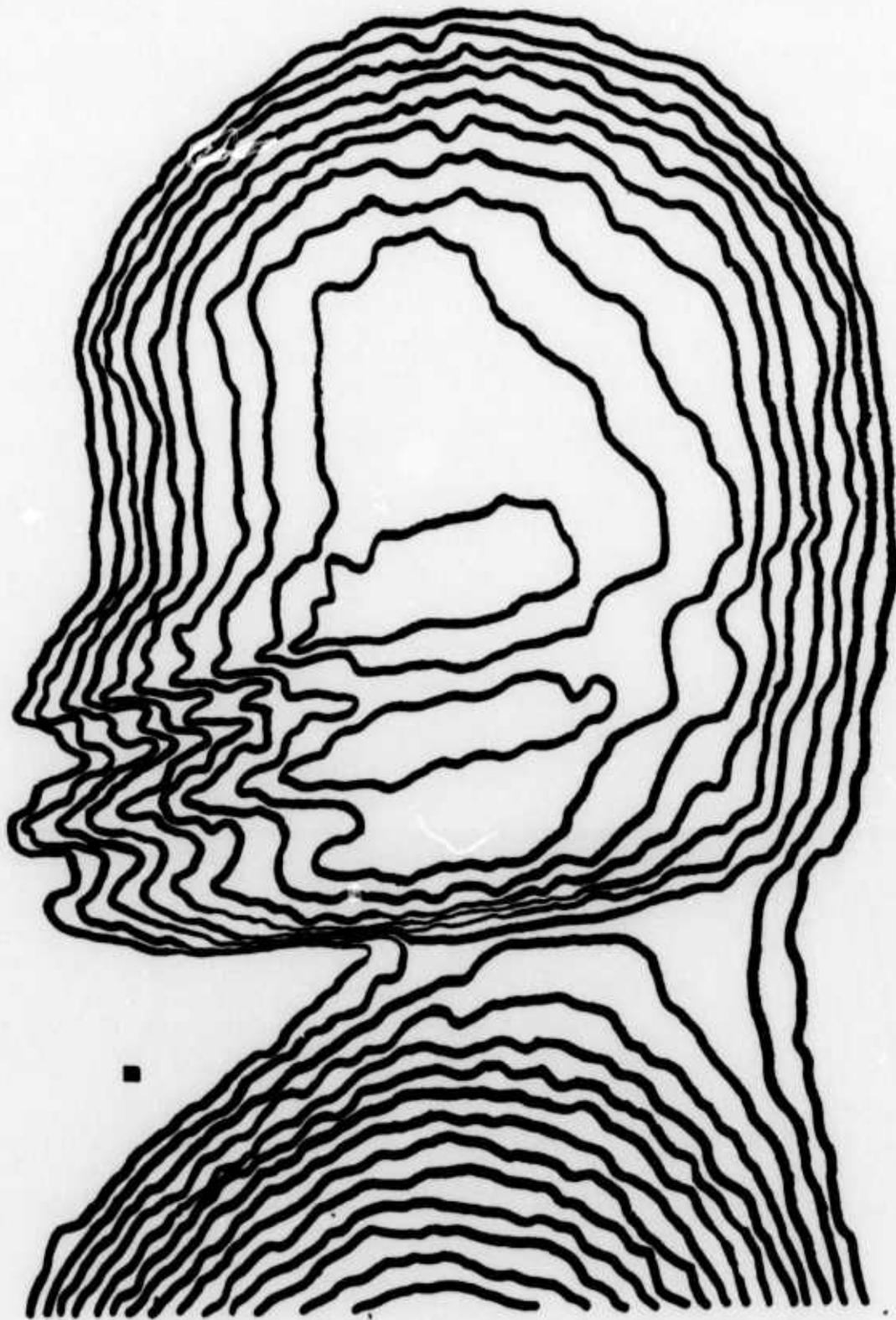
A-7   Light contour tracing of right view. A-5 and A-6 produced a
       slight three dimensional effect but did not yield any depth
       information.
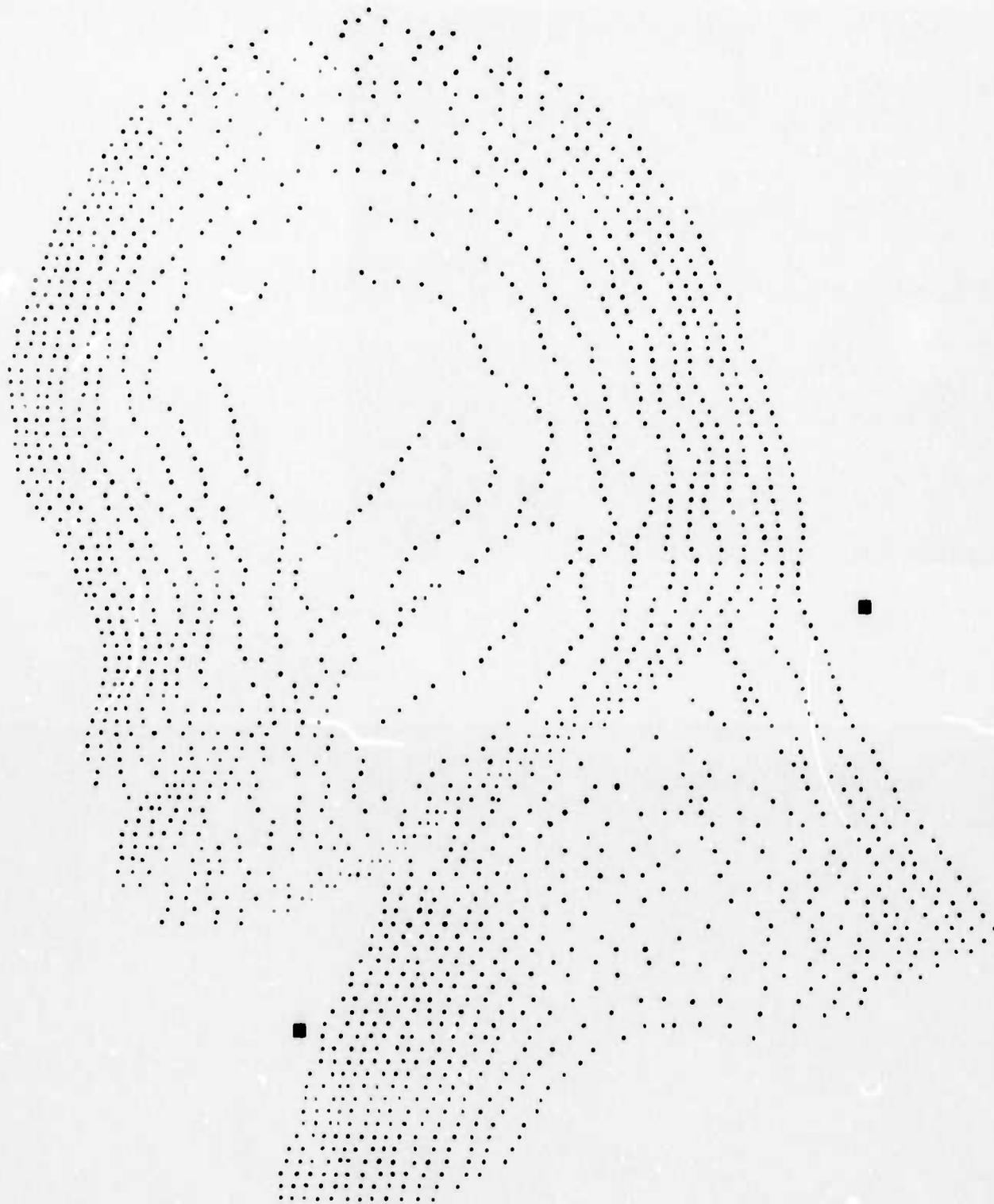
A-9   Dotted contour tracing of right view. This type of contour
      was not any improvement over set A-5, A-6.

FRAME 2

FRAME 1

A-10 Two More Frame's From the Spruce Footage
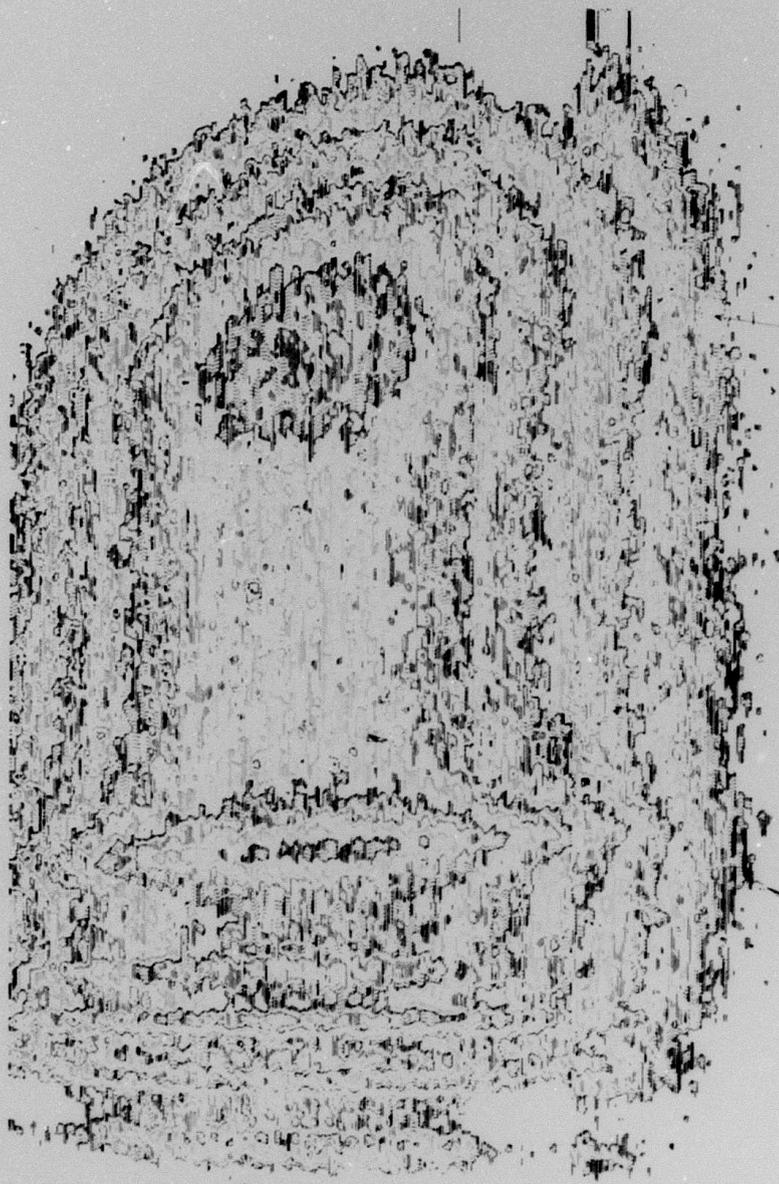
DATE _9-7-72_ RECORDING NO. _I L_ IDENTIFICATION _LEFT, 1st VIEW_

SPOT HEIGHT _1mm_	WEDGE NUMBER _____	RATIO ARM _20:1_	OPERATOR _____
SPOT WIDTH _1mm_	Δ D INCREMENT _____		COMMENTS: _____
OBJECTIVE _x6 /_	TABLE SPEED _20 in/min_	RECORD SPACING _375μ_	_____
CONDENSER _x /_	PEN DAMPING _10+_	SAMPLE SPACING _18.75μ_	_____

A-11 Left isodensity contour made from left A-10 frame.
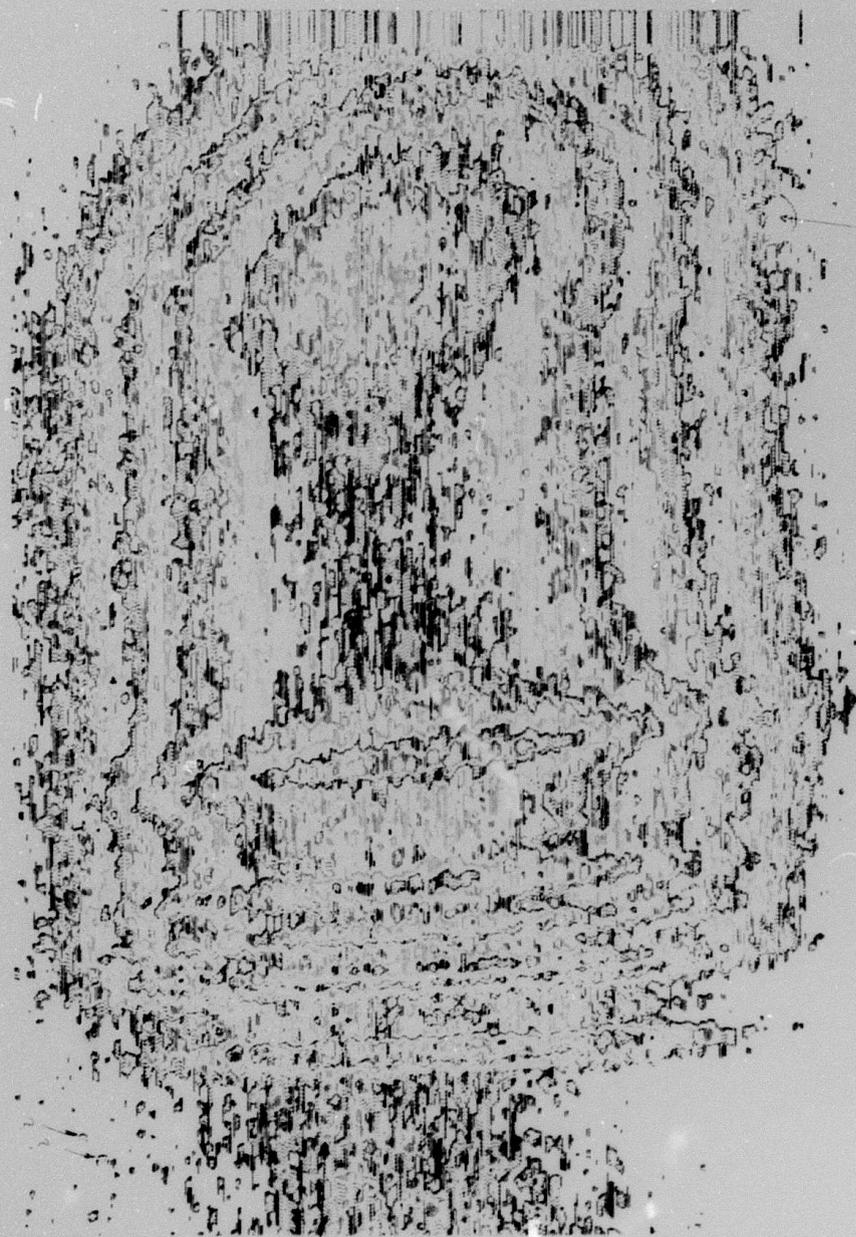
DATE 9-7-72   RECORDING NO. "I·R"   IDENTIFICATION RIGHT, 1ST VIEW

SPOT HEIGHT 1mm   WEDGE NUMBER _____   RATIO ARM 20:1   OPERATOR _____
SPOT WIDTH 1mm   Δ D INCREMENT _____   COMMENTS: _____
OBJECTIVE X6 /   TABLE SPEED 20 in/min   RECORD SPACING 375μ _____
CONDENSER X /   PEN DAMPING 10+   SAMPLE SPACING 18.75μ _____

A-12 Right isodensity contour made from right A-10 frame.